

OPEN ACCESS

EDITED BY

Suranjoy Singam,
University of Guelph, Canada

REVIEWED BY

Noemi Elisabet Zaritzky,
National University of La Plata, Argentina
Vivek Kambhampati,
National Institute of Technology
Rourkela, India

*CORRESPONDENCE

Zhihao Zhao
✉ zhaozhiao1991@163.com
Jie Pang
✉ pang3721941@163.com
Mingwei Zhang
✉ mwzhh@vip.tom.com

RECEIVED 17 February 2025

ACCEPTED 21 April 2025

PUBLISHED 13 May 2025

CITATION

Lin Z, Zhao Z, Zhou P, Deng Y, Liu G, Li P,
Zeng J, Xiang F, Pang J and Zhang M (2025)
Physicochemical properties of peanut oil
body nutritional emulsions: effects of energy
density and nutrient ratio.
Front. Sustain. Food Syst. 9:1578053.
doi: 10.3389/fsufs.2025.1578053

COPYRIGHT

© 2025 Lin, Zhao, Zhou, Deng, Liu, Li, Zeng,
Xiang, Pang and Zhang. This is an
open-access article distributed under the
terms of the [Creative Commons Attribution
License \(CC BY\)](https://creativecommons.org/licenses/by/4.0/). The use, distribution or
reproduction in other forums is permitted,
provided the original author(s) and the
copyright owner(s) are credited and that the
original publication in this journal is cited, in
accordance with accepted academic practice.
No use, distribution or reproduction is
permitted which does not comply with these
terms.

Physicochemical properties of peanut oil body nutritional emulsions: effects of energy density and nutrient ratio

Zihui Lin^{1,2,3}, Zhihao Zhao^{2,3*}, Pengfei Zhou², Yuanyuan Deng²,
Guang Liu², Ping Li², Jiarui Zeng², Fahui Xiang³, Jie Pang^{1*} and
Mingwei Zhang^{2*}

¹College of Food Science, Fujian Agriculture and Forestry University, Fuzhou, China, ²Sericultural & Agri-Food Research Institute Guangdong Academy of Agricultural Sciences/Key Laboratory of Functional Foods, Ministry of Agriculture and Rural Affairs/Guangdong Key Laboratory of Agricultural Products Processing, Guangzhou, China, ³Fujian Key Laboratory of Agro-products Quality & Safety, Fuzhou, China

The physical and chemical stability of peanut oil body (POB) nutritional emulsions and traditional emulsifier-based nutritional emulsions were compared under varying energy densities and nutrient ratios, with a focus on protein adsorption at the oil-water interface. The results demonstrated that flocculation was the primary instability mechanism for POB emulsions, whereas emulsifier-based emulsions predominantly experienced coalescence. At energy densities of 1.9 and 2.1 kcal/mL, POB nutritional emulsions exhibited lower PDI values (0.136 and 0.139), compared to emulsifier-based emulsions (0.152 and 0.191). Additionally, micromorphology analysis indicated enhanced anti-coalescence properties for POB emulsions. The interfacial protein adsorption capacity of POB emulsions (6.8 and 7.0 mg/m²) was also lower than that of emulsifier-based emulsions (7.5 and 8.0 mg/m²), suggesting that the thinner interfacial protein film may contribute to the improved storage stability of POB emulsions. At an energy density of 2.1 kcal/mL, after adjusting the nutrient ratio, the CI values of POB emulsions (8.79%, 3.95%, 3.75%) were consistently lower than those of emulsifier-based emulsions (10.25%, 8.16%, 8.02%), further indicating superior storage stability. Both emulsions showed similar appearance colors. These findings demonstrate that POB emulsions offer a promising alternative to refined oil in nutritional emulsion formulations, effectively replacing traditional emulsifiers, particularly in high-energy-density applications.

KEYWORDS

peanut oil body, emulsion, energy density, nutrient ratio, interfacial protein adsorption, stability

1 Introduction

Nutritional emulsions, as oil-in-water (O/W) emulsion systems enriched with various nutrients, are widely utilized in formula foods designed for special medical purposes. They effectively address the nutritional requirements of patients with eating restrictions and digestive or absorption disorders (Qu et al., 2024). However, the thermodynamic instability of the O/W emulsion system, compounded by the high nutrient content of nutritional emulsions, often leads to issues such as fat separation and protein coagulation. To enhance stability and prolong shelf life, food emulsifiers are commonly added during

production (Ravera et al., 2021). Emulsifiers contain a hydrophobic tail and a hydrophilic head. This structure enables them to form stable films at the oil-water interface, which promote emulsion formation and improve physical stability by reducing interfacial free energy. Among various emulsifiers, synthetic emulsifiers, such as polyol fatty acid esters, exhibit excellent emulsifying properties and are widely utilized in the food industry, including in nutritional emulsion products (Arancibia et al., 2017). However, an increasing number of studies suggest that synthetic emulsifiers may contribute to the rising incidence of various diseases, such as Crohn's disease, allergies, and autoimmune disorders. These conditions are associated with impaired intestinal barrier function and changes in gut microbiota composition (Csáki, 2011; Lerner and Matthias, 2015). Additionally, synthetic emulsifiers may enhance the absorption of foodborne pollutants, potentially aggravating conditions related to autoimmune diseases (Chassaing et al., 2015; Abu-Qare et al., 2003). To address these concerns, the food industry is actively exploring green, safe alternatives to synthetic emulsifiers or developing entirely new products with naturally derived ingredients (McClements et al., 2017).

Oil bodies (OB) are spherical subcellular organelles in plants specialized for lipid storage. Their core consists of triglycerides, surrounded by a single-layer membrane composed of proteins and phospholipids (Bonsegna et al., 2011). This unique structure provides OB with natural pre-emulsification properties, enabling them to form natural O/W emulsions without the need for added emulsifiers or homogenization steps (Zaaboul et al., 2022). Beyond lipids and proteins, OB are abundant in phytochemicals such as vitamin E and phytosterols, positioning them as a promising alternative to refined vegetable oils in the emulsified food (Shi et al., 2024). Recent studies have explored the application of OB as fat substitutes in various foods, including ice cream (Zaaboul et al., 2024), yogurt (Dou et al., 2022), and mayonnaise (Mert and Vilgis, 2021). Furthermore, OB demonstrate desirable processing characteristics, exhibiting stability in physicochemical properties under conditions such as high-pressure homogenization and heat treatment (Gao et al., 2022). These findings suggest that OB represent a promising option as an oil substitute in nutritional emulsions, potentially eliminating the need for food emulsifiers.

Lipids, proteins, and carbohydrates, as the primary energy sources in nutritional emulsions, collectively play critical roles in supporting normal physiological functions by providing energy, supplementing nutrition, and regulating metabolism. Nutritional emulsions based on these three nutrients are mainly applied to patients with oral intake difficulties, digestive and absorption disorders, or symptoms of malnutrition such as weight loss, edema, or anemia (Wali et al., 2025). The dosage of nutritional emulsions can be tailored to the specific symptoms of patients with special conditions. For instance, while most patients can tolerate sufficient doses, those with severe conditions like post-gastrectomy may struggle to achieve adequate intake (Furuta et al., 2023). Thus, different symptoms necessitate nutritional emulsions with varied energy densities to accommodate the specific metabolic requirements of patients. The energy density of a nutritional emulsion is determined by the composition of the three primary nutrients, with standard caloric values of 9 kcal/g for lipids and 4 kcal/g for both proteins and carbohydrates (Yuan et al., 2024). Currently, most studies on nutritional emulsions

address formulations with energy densities ranging from 1.0 to 1.5 kcal/mL, as these values are suitable for a majority of patient needs (Yamazaki et al., 2023). Additionally, patients with different types of diseases may require adjustments in the nutrient composition and ratios of nutritional emulsions to meet their specific nutritional needs without compromising sufficient energy supply (Cawood et al., 2012).

In this study, the novel nutritional emulsions, free of synthetic emulsifiers and with varying nutrient densities and composition ratios, were prepared based on the natural emulsifying properties of peanut OB. Their basic characteristics, including particle size, ζ -potential, microstructure, and apparent viscosity, were analyzed. Emulsification properties were evaluated based on the adsorption behavior of interfacial proteins, while storage stability was assessed using the creaming index. The results were also compared with those of traditional nutrient emulsions stabilized by food emulsifiers. The purpose of this study is to investigate the feasibility of preparing the novel emulsifier-free nutrient emulsions based on OB and the effect of nutrient density and composition ratio on their stability. The findings offer a novel approach to the development of more natural and healthy nutritional emulsions, while also promoting the broader application of OB in food emulsion systems.

2 Materials and methods

2.1 Materials

Peanuts were purchased from a local supermarket. Peanut oil purchased from Yihai Kerry Food Marketing Co., Ltd. Sodium caseinate (purity: 99%) was purchased from Xinjiang Meihua Amino Acid Co., Ltd. Maltodextrin (DE value 15–20) was purchased from Qinquangdao Lihua Starch Co., Ltd. Phospholipids, sucrose fatty acid esters, and monoglycerin and diglyceride fatty acid esters were purchased from Masson Technology Co., Ltd. All other reagents are analytical grade.

2.2 Extraction of peanut oil body

Peanut oil body (POB) was extracted using a water extraction method. Mature peanuts were soaked in deionized water (1:7, w/w) at 4°C for 10 h, then processed in a high-speed blender for 2 min. The resulting peanut slurry was filtered through four layers of gauze, and the filtrate was centrifuged at 10,000 × g for 20 min at 4°C. The POB was collected from the upper layer. Fresh POB was determined to be composed of 67.84% lipid, 1.60% protein, and 20.61% moisture using Soxhlet extraction method, Kjeldahl nitrogen determination method, and direct drying method, respectively.

2.3 Preparation of nutritional emulsion

2.3.1 Preparation of nutritional emulsion from POB

Quantitative amounts of sodium caseinate and maltodextrin were dissolved in water, followed by the addition of POB with

thorough stirring. The mixture was then homogenized using a high-speed shear homogenizer (IKA-T25, Germany) at 10,000 rpm for 5 min. Subsequently, it was processed in a high-pressure homogenizer (AH-BASICI, ATS ENGINEERING, CA) at 50 MPa for two cycles. Finally, the emulsion was sterilized at 121°C for 15 min and cooled to room temperature to obtain the POB nutritional emulsion (POBNE).

2.3.2 Preparation of nutritional emulsion from peanut oil and emulsifier

Quantitative amounts of phospholipids and fatty acid esters were added to a measured amount of peanut oil and heated in a water bath at 65°C while stirring at 1,000 rpm using a rotor. The mixture was heated for 30 min until the emulsifiers were completely dissolved in the oil phase. Meanwhile, the probe of a high-speed shear homogenizer was placed into the aqueous phase containing dissolved sodium caseinate and maltodextrin, and the speed was set to 3,000 rpm. The oil phase with dissolved emulsifiers was then slowly poured into the aqueous phase while mixing, ensuring complete combination of the two phases. The speed was then increased to 10,000 rpm for 5 min. The high-pressure homogenization and high-temperature sterilization steps were performed in the same manner as for POBNE. After cooling, the peanut oil nutritional emulsion (PONE) was obtained.

2.3.3 Energy density setting in nutritional emulsions

In this experiment, sodium caseinate, oil (POB or pure peanut oil) and maltodextrin were used as the main energy sources of emulsion. According to the energy provided by the three nutrients, the energy density of emulsion can be calculated. By changing the concentration of various nutrients in the system, the energy density of nutritional emulsion can be set to 0.7, 1.0, 1.3, 1.6, 1.9, 2.1 kcal/mL, respectively. The formulation of emulsion is

shown in Table 1. The energy density (ED) was calculated using the following formula:

$$ED \left(\frac{\text{kcal}}{\text{mL}} \right) = \frac{m_p \times 4 + m_l \times 9 + m_c \times 4}{1000} \quad (1)$$

Where m_p represents the mass of protein (g/L), m_l represents the mass of lipids (g/L), m_c represents the mass of carbohydrates (g/L).

2.3.4 Energy ratios setting in nutritional emulsions

This experiment designed three different types of nutrition emulsion according to the ratios of energy provided by protein, lipid and carbohydrate and the nutritional requirements of patients with different special diseases:

The energy ratios of high lipid type (HLT) is 17% protein, 50% lipids, and 33% carbohydrates. The energy ratios of general type (GT) is 17% protein, 38% lipids, and 45% carbohydrates. The energy ratios of high carbohydrate type (HCT) is 17% protein, 26% lipids, and 57% carbohydrates. The formulation of emulsion is shown in Table 2.

2.4 Physical stability of emulsion

2.4.1 Particle size and ζ -potential

Dilute the sample with deionized water in a ratio of 1:800, and measure the particle size and ζ -potential of emulsion through ZSE Malvern nanoparticle particle size and potential analyzer. The average particle size of droplets is expressed by the average volume diameter ($D_{4,3}$). The refractive index of emulsion and dispersed phase (deionized water) is set to 1.45 and 1.33 respectively. All samples were tested at 25°C.

TABLE 1 The composition of nutritional emulsions at different energy densities.

Sample	Energy density (kcal/mL)	POB/g	PO/g	SC/g	MD/g	PL/mg	SE/mg	MDE/mg	DI/mL
POBNE	0.7	57.3	–	28.9	57.8	–	–	–	988.2
	1.0	82.0	–	41.2	82.5	–	–	–	983.1
	1.3	106.4	–	53.6	107.3	–	–	–	978.1
	1.6	131.0	–	65.9	132	–	–	–	973.0
	1.9	155.7	–	78.3	156.8	–	–	–	967.9
	2.1	172.0	–	86.5	173.3	–	–	–	964.6
PONE	0.7	–	38.9	29.8	57.8	61	168.5	168.5	1,000
	1.0	–	55.6	42.5	82.5	87	240.5	240.5	1,000
	1.3	–	72.2	55.3	107.3	113	312.5	312.5	1,000
	1.6	–	88.9	68	132	139	384.5	384.5	1,000
	1.9	–	105.6	80.8	156.8	165	457	457	1,000
	2.1	–	116.7	89.3	173.3	182.5	505	505	1,000

POBNE, peanut oil body nutritional emulsion; PONE, peanut oil nutritional emulsion; SC, sodium caseinate; MD, maltodextrin; PL, phospholipids; SE, sucrose fatty acid esters; MDE, monoglycerin and diglyceride fatty acid esters; DI, deionized water.

TABLE 2 The composition of nutritional emulsions at different nutrient ratios.

Sample	Type	POB/g	PO/g	SC/g	MD/g	PL/mg	SE/mg	MDE/mg	DI/mL
POBNE	HLT	172.0	–	86.5	173.3	–	–	–	964.6
	GT	130.6	–	87.2	236.3	–	–	–	973.1
	HCT	89.5	–	87.9	299.3	–	–	–	981.6
PONE	HLT	–	116.7	89.3	173.3	182.5	505	505	1,000
	GT	–	88.6	89.3	236.3	138.5	384.5	384.5	1,000
	HCT	–	60.7	89.3	299.3	94.7	262.8	262.8	1,000

POBNE, peanut oil body nutritional emulsion; PONE, peanut oil nutritional emulsion; SC, sodium caseinate; MD, maltodextrin; PL, phospholipids; SE, sucrose fatty acid esters; MDE, monoglycerin and diglyceride fatty acid esters; DI, deionized water.

2.4.2 Microstructure

The micromorphology of the emulsion sample was examined using an optical microscope (MSHOT-ML51-M) equipped with a 10 × eyepiece and a 40 × objective lens. A 4 μL sample was placed onto a glass slide, covered with a coverslip, and carefully checked to ensure no air bubbles were present. After allowing the sample to stand for 5 min, observations were conducted.

2.4.3 Apparent viscosity

Accurately transfer 1.4 mL of sample to the sample table of the rheometer (HR-1, TA, USA), and use a clamp with a diameter of 40 mm for contact measurement. Set the distance between the sample table and the fixture to 1,000 μm, and measure the static shear viscosity of the sample. The time for increasing the shear rate from 0.1 to 100 s⁻¹ is 1 min. All samples were measured at 25°C.

2.4.4 Dynamic stability

The turbiscan stability index (TSI) was measured using a multiple light scattering instrument (Turbiscan Lab stability analyzer). Transfer the quantitative sample to the sample tube of the instrument and ensure that the sample has no wall contact or bubbles. The sample tube was then placed in the analysis chamber. The scanning time was set for 1 h, with scans taken every 100 s. All measurements were performed at 25°C.

2.4.5 Creaming index (CI)

A 3 mL emulsion sample was transferred to a glass bottle and stored in a sealed container at 25°C for 15 days. The total height of emulsion and the thickness of emulsion layer were calculated by single scanning analysis of emulsion through Turbiscan Lab stability analyzer. The CI was calculated using the following formula:

$$CI (\%) = \frac{h_1}{h_0} \times 100\% \quad (2)$$

Where h_0 represents the total height of the emulsion and h_1 represents the thickness of the emulsion layer.

2.5 Interfacial protein adsorption

The adsorption capacity and rate of interfacial protein were determined using the method of Shen et al., with slight modifications (Shen et al., 2024). The emulsion was centrifuged at 35,000 × g at 4°C for 1 h. The bottom fraction was collected using a syringe, and the protein concentration in the bottom fraction was determined using a BCA protein assay kit (E8053-500T, Shanghai Titan Scientific Co., Ltd.). The standard curve for the BCA protein assay kit is $y = 1.358x + 0.1185$, $R^2 = 0.99$, where x is the absorbance and y is the protein concentration. The interfacial protein adsorption rate was calculated according to the following formula:

$$AP (\%) = \frac{C_0 - C_t}{C_0} \times 100\% \quad (3)$$

Where C_0 denotes the initial protein concentration of the emulsion (40 mg/mL), and C_t denotes the protein concentration of the bottom fraction after centrifugation.

The amount of protein adsorbed at the emulsion interface was calculated using the following formula:

$$\Gamma \left(\frac{\text{mg}}{\text{m}^2} \right) = \frac{(C_0 - C_t) \times D_{3,2}}{6\varphi} \quad (4)$$

Where Γ denotes the amount of interfacial protein adsorbed (mg/m²), C_0 and C_t have the same meanings as in the previous formula, $D_{3,2}$ are measured by laser particle size analyzer (Bettersize2600, Dandong Baite Instrument Co., Ltd.) to indicate the average diameter of emulsion area, and φ denotes the volume fraction of the oil phase in the emulsion (0.03).

2.6 Color analysis

The color of emulsion is measured and analyzed by a colorimeter (CM-700d, Huidong instrument equipment Co., Ltd), using the CIE color chromaticity L^* , a^* , and b^* scales (L^* = dark/light, a^* = red/green, b^* = yellow/blue). The higher the L^* value of emulsion color is, the brighter the color is; the higher the a^* value is, the redder the emulsion color is; the higher the b^* value is, the yellower the color is; and the color difference value ΔE^* of the sample is calculated by the formula:

$$\Delta E^* = \sqrt{(L^* - L_0)^2 + (a^* - a_0)^2 + (b^* - b_0)^2} \quad (5)$$

Where L_0 , a_0 , and b_0 represent the chromaticity of the whiteboard ($L_0 = 93$, $a_0 = 0$, $b_0 = 3.6$).

2.7 Statistical analysis

All samples were assayed at least three times, with precision between data indicated by error bars. Statistical analysis was performed using the analysis of variance (ANOVA) procedure in MATLAB. Differences in mean values were detected using the least significant difference test ($p < 0.05$).

3 Results and discussion

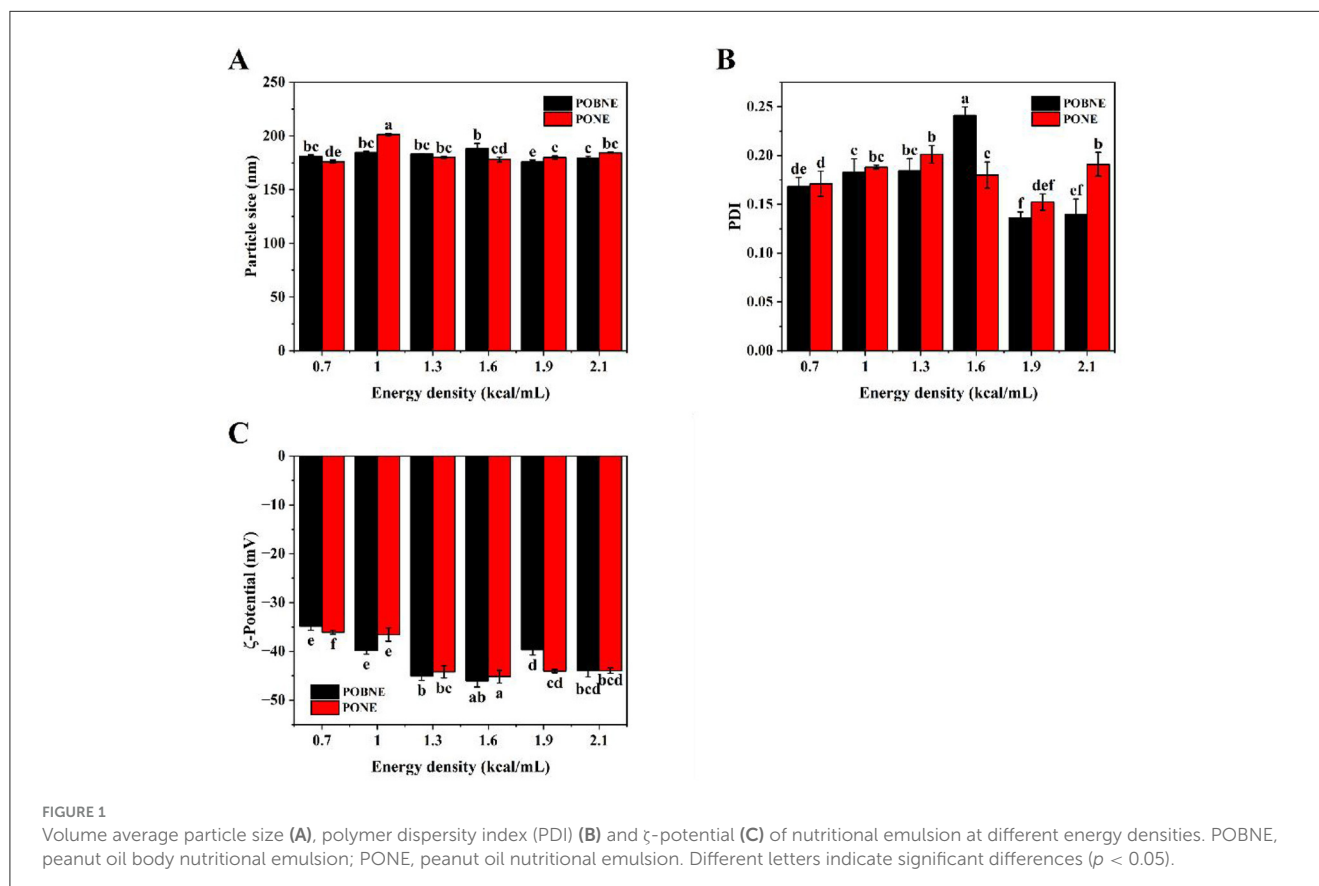
3.1 Effect of energy density on emulsion properties

3.1.1 Particle size and ζ -potential

The relationship between emulsion particle size and energy density is shown in Figure 1A. The PONE with an energy density of 1.0 kcal/mL exhibited the largest particle size (201.2 ± 1.4 nm), while the particle sizes of other emulsions were below 200 nm. The results indicated that the particle size of POBNE was smaller than that of PONE at energy densities of 1.0, 1.9, and 2.1 kcal/mL. The results demonstrated that OB has certain advantages in preparing nutrient emulsions at higher energy densities. The PDI values shown in Figure 1B further support this conclusion. Under high

energy densities (1.9 and 2.1 kcal/mL), POBNE had smaller PDI values (0.14 ± 0.01 , 0.14 ± 0.02) compared to PONE (0.15 ± 0.01 , 0.19 ± 0.03), indicating that OB emulsions prepared under high energy densities had a more uniform particle size distribution and higher physical stability, consistent with the particle size results. In emulsion systems with complex compositions, emulsions formed at relatively high component concentrations showed better stability, which may be related to the substances involved in the emulsification process (Yu et al., 2025). Similarly, Yang et al. reported that emulsions prepared with orange peel pectin and sodium caseinate exhibited smaller droplet sizes at higher pectin and protein concentrations (Yang et al., 2023). These experimental results suggest that higher energy densities promote the formation of stable emulsions.

The ζ -potential is a critical parameter for assessing the local charge distribution in emulsions. A higher absolute value of ζ -potential indicates stronger repulsive forces between droplets, which helps prevent droplet aggregation and enhances emulsion stability. As shown in Figure 1C, the absolute ζ -potential values of all emulsions exceed 30 mV, suggesting strong electrostatic repulsion between droplets and a stable emulsion system (Diao et al., 2024). The results demonstrate that the absolute ζ -potential of the emulsions initially increases and then decreases with rising energy density. Notably, both POBNE and PONE exhibit the highest absolute ζ -potential values at an energy density of 1.6 kcal/mL (45.0 ± 1.1 mV and 46.7 ± 0.6 mV, respectively), indicating significant electrostatic repulsion between droplets. This increase in ζ -potential may be attributed to the



exposure of more hydrophobic side chains in proteins under these conditions (Yu et al., 2024). However, at higher energy densities, the absolute ζ -potential decreases. This reduction may result from the presence of excess proteins in the system, which can cover hydrophobic groups on the droplet surfaces and form an electrostatic shield, thereby lowering the ζ -potential (Ren et al., 2018). Consequently, higher energy densities may promote protein aggregation and weaken the electrostatic repulsion between emulsion droplets.

3.1.2 Microstructure

The microstructure of each emulsion was observed using an optical microscope, and the results are presented in Figure 2. The observations reveal that the droplets in all emulsion groups are evenly dispersed. As energy density increases, the droplets become more densely packed. This is because, under the same homogenization conditions, the increased oil content (dispersed phase) in the system leads to the formation of more droplets. However, at higher energy densities, the emulsions exhibit signs

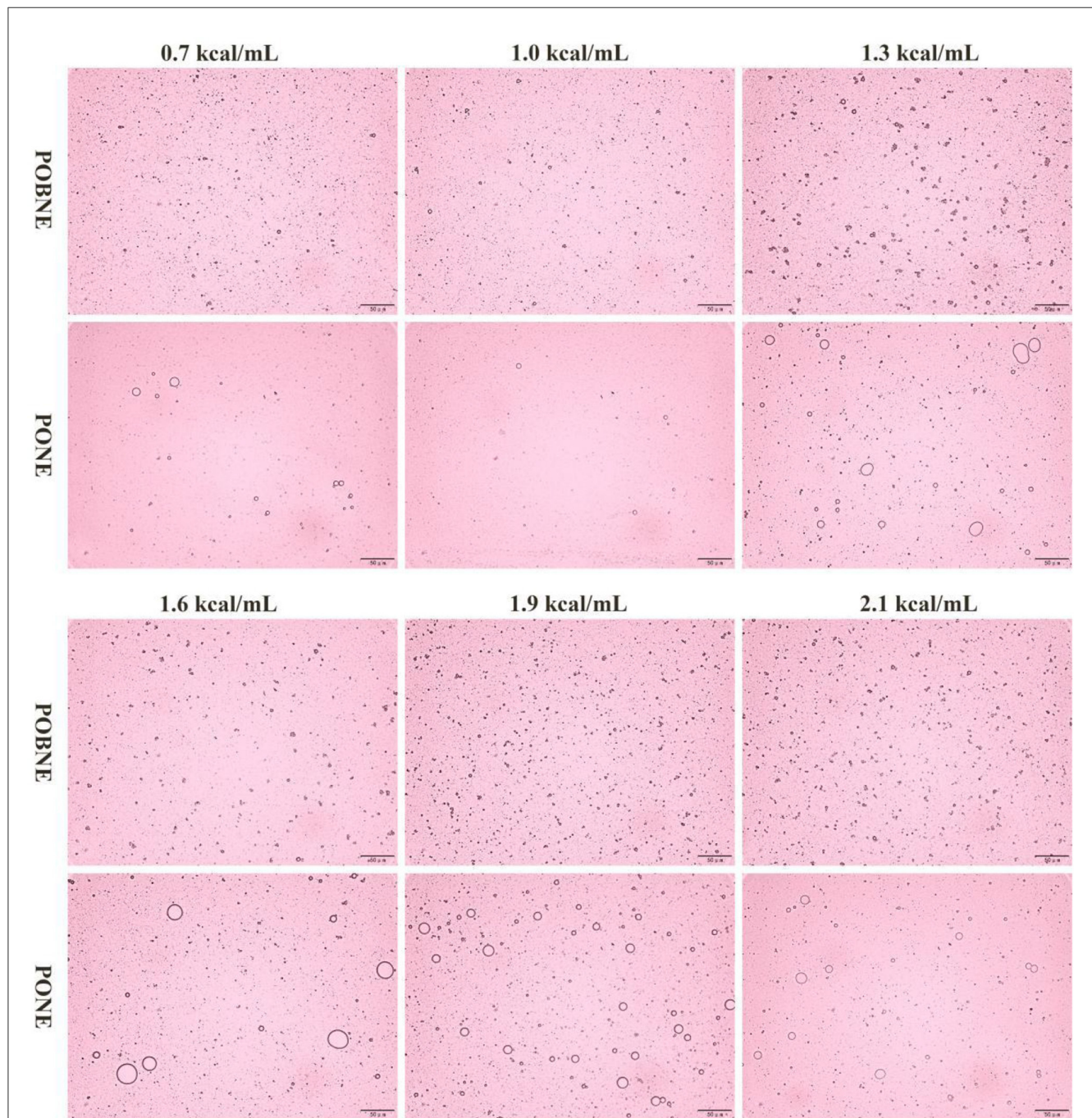


FIGURE 2
Microstructure of nutritional emulsion at different energy densities. POBNE, peanut oil body nutritional emulsion; PONE, peanut oil nutritional emulsion.

of instability. This instability is primarily attributed to Brownian motion, which facilitates droplet collisions. As the number of droplets in the system increases, the likelihood of such collisions rises, accelerating the occurrence of instability phenomena such as flocculation and coalescence. Interestingly, the instability mechanisms differ between emulsions. The POBNE predominantly exhibits flocculation, characterized by droplet agglomeration, whereas the PONE shows coalescence, where smaller droplets merge to form larger ones. Oleosin, the primary protein on the surface of oil bodies, plays a crucial role in maintaining the integrity and stability of oil bodies. Its high interfacial activity effectively inhibits droplet coalescence (Guzha et al., 2023). These findings indicate that higher energy densities promote emulsion instability. Additionally, nutrient emulsions prepared from POB demonstrate a reduced tendency for droplet coalescence, highlighting their potential for improving emulsion stability.

3.1.3 Apparent viscosity

The variation in apparent viscosity of each emulsion group with shear rate (1–100 s^{-1}) is shown in Figure 3. As the shear rate increases, the viscosity of the emulsions decreases, indicating that all emulsions exhibit shear-thinning behavior characteristic of pseudoplastic fluids. This phenomenon is primarily attributed to the disruption of aggregates or the unwinding of flocculated structures along the flow direction (Kang et al., 2023). The results show that the emulsions reach their maximum apparent viscosity at an energy density of 2.1 kcal/mL. Typically, higher concentrations lead to increased apparent viscosity, which is mainly due to interfacial adsorption and restricted molecular motion. As energy density increases, the concentration of nutrients in the emulsion system rises, with significant amounts of sodium caseinate and maltodextrin dissolving in the water phase. This results in a sharp increase in the density and consistency of the water phase, making it more difficult for small droplets in the oil phase to move within the system (Li et al., 2020). Additionally, the increased oil content leads to a higher number of droplets in the system, reducing the spacing between droplets and further restricting the movement of small droplets (Kong et al., 2025). Moreover, under the same energy density, the viscosity curves of POBNE and PONE are nearly identical, indicating that nutrient emulsions prepared from POB exhibit rheological properties comparable to those of emulsions stabilized with synthetic emulsifiers.

3.1.4 Interface protein of emulsion

The adsorption behavior of proteins at the oil-water interface is critical to the stability and rheological properties of emulsion systems (Liu et al., 2024). The interfacial protein adsorption rate (AP) for each emulsion is shown in Figure 4A. As energy density increases, the AP value of the emulsions rises. This is primarily due to the higher protein concentration in the system, which promotes the formation of a viscoelastic film around the oil droplets, thereby stabilizing the emulsion (Kim et al., 2020). Additionally, the increase in droplet number leads to a larger total oil-water interfacial area, allowing more proteins to participate in emulsification. As more proteins adsorb at the oil-water interface, the friction between droplets increases, contributing to

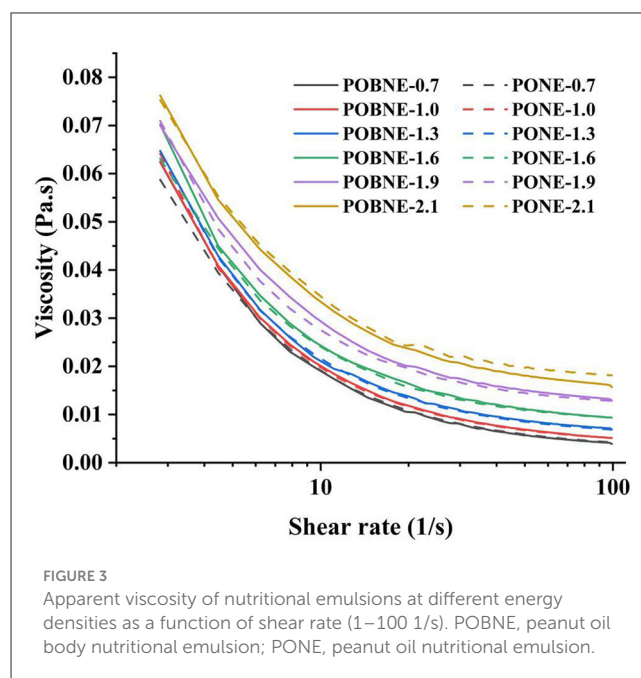
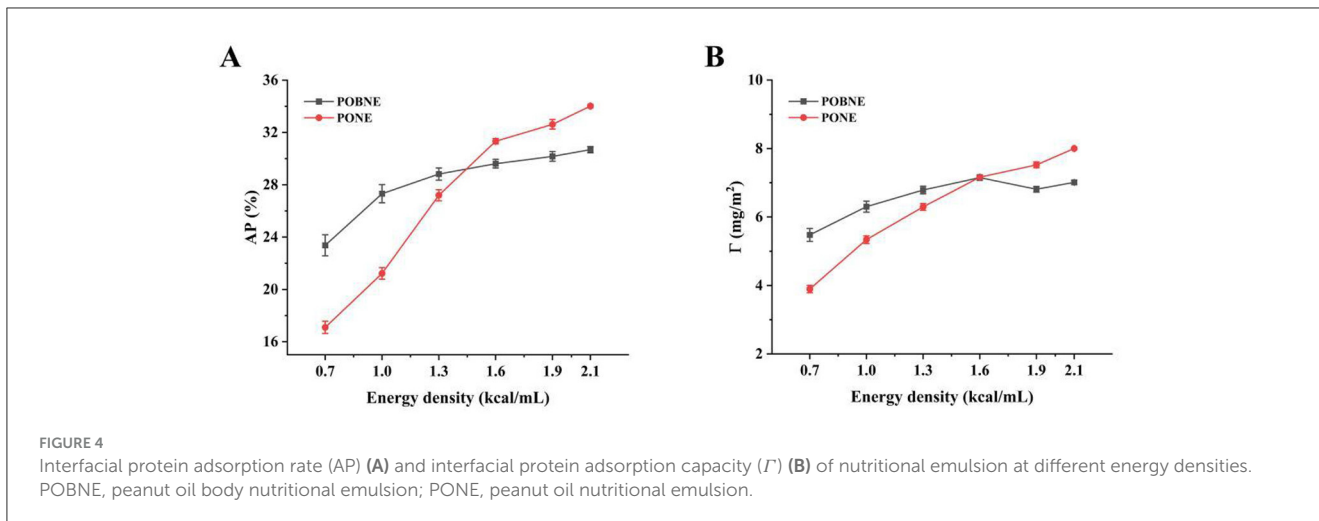


FIGURE 3
Apparent viscosity of nutritional emulsions at different energy densities as a function of shear rate (1–100 1/s). POBNE, peanut oil body nutritional emulsion; PONE, peanut oil nutritional emulsion.

the observed rise in emulsion viscosity, which aligns with the previously discussed changes in apparent viscosity. The results indicate that at lower energy densities (0.7–1.3 kcal/mL), the AP value of POBNE is higher than that of PONE. However, as energy density continues to increase, the AP value of PONE gradually surpasses that of POBNE. This difference may be attributed to the types of proteins involved in emulsification. Proteins with higher stability tend to exhibit faster adsorption rates at oil-water interfaces of the same polarity (Zhang et al., 2022). When POB are used in nutritional emulsions, their unique pre-emulsified structure includes a protein film, primarily composed of oleosin, prior to emulsification. Although homogenization disrupts the protein film structure and refines the OB, oleosin remains on the droplet surface, maintaining emulsion stability and participating in emulsification alongside other proteins (Schröder et al., 2017; Lin et al., 2025). Compared to PONE, the oil-water interface of POBNE, which contains oleosin, can adsorb proteins more rapidly, promoting faster saturation of proteins at the interface and enhancing emulsion stability (Sun et al., 2023). As energy density increases, the AP value of POBNE gradually stabilizes, while the AP value of PONE continues to rise. This suggests that at higher energy densities, the POBNE interface approaches saturation with less protein adsorption, forming a stable emulsion system. In contrast, under the same conditions, PONE requires continued protein adsorption to achieve comparable stability.

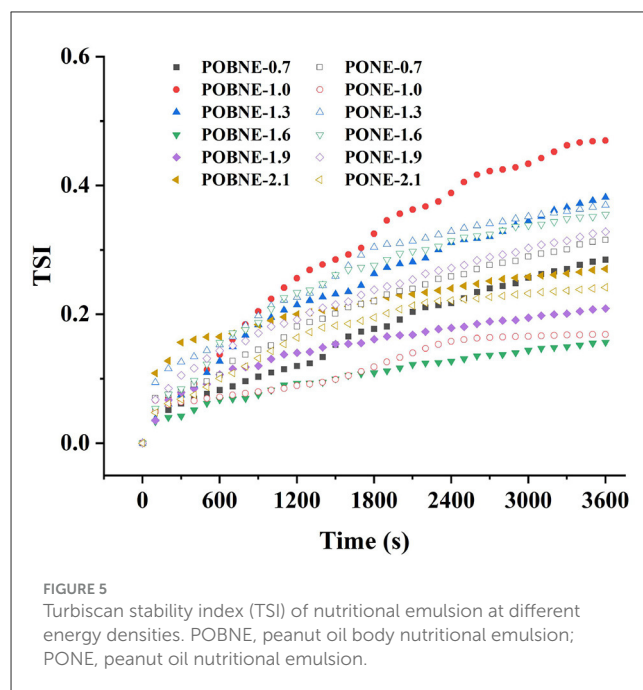
The interfacial protein adsorption capacity (Γ) of the emulsions is shown in Figure 4B. The results indicate that as energy density increases, the amount of interfacial protein adsorption also increases. This suggests that the thickness of the interfacial protein film on the droplet surface grows, enhancing the protection of oil droplets and contributing to emulsion stability. Notably, when the energy density exceeds 1.6 kcal/mL, the interfacial protein adsorption of POBNE plateaus, indicating that the protein adsorption at the emulsion interface has reached saturation. This



corresponds to a highly stable emulsion system, consistent with the earlier findings on protein adsorption rate. In contrast, the interfacial protein adsorption capacity of PONE continues to increase and surpasses that of POBNE, suggesting that the protein film formed at the oil-water interface in PONE is thicker and capable of adsorbing more proteins (Zhang et al., 2021). However, microstructural analysis reveals that PONE at higher energy densities is more susceptible to droplet coalescence, suggesting that its thicker interfacial film lacks sufficient strength. Upon droplet collisions, the film is easily compromised, leading to reduced emulsion stability. Conversely, although the interfacial film formed by POBNE is thinner, it exhibits better structural integrity. After droplet collisions, the droplets in POBNE maintain smaller particle sizes and preserve their structural integrity, which supports emulsion stability. The results show that when the energy density of POBNE reaches 1.6 kcal/mL, the interfacial protein adsorption capacity saturates at 7.01 ± 0.06 mg/m². Even at higher energy densities, POBNE forms a thinner but denser interfacial protein film compared to PONE, which contributes to its superior stability.

3.1.5 Storage stability

The TSI of each emulsion is shown in Figure 5. Normally, the smaller TSI indicates higher stability of emulsion. The results showed that the TSI of each emulsion were <0.5 with the change of scanning time, indicating that they had high stability. In both POBNE and PONE samples, emulsions with low and high energy density exhibited lower terminal TSI values, while emulsions with medium energy density showed the highest terminal TSI values. In POBNE, the 1.0 and 1.3 kcal/mL samples had the highest and second-highest TSI values, respectively, while in PONE, the 1.3 and 1.6 kcal/mL samples had the highest and second-highest TSI values, respectively. Since the TSI scanning time was relatively short, we further analyzed the stability of each emulsions over a longer storage period using the creaming index. The CI is a direct indicator of fat separation during storage and is commonly used to evaluate the storage stability of emulsions. Figure 6 illustrates the CI of different emulsion stored at room temperature (25°C) for 15 days. As energy density increased, the CI of POBNE initially



showed an upward trend followed by a decline, whereas the CI of PONE exhibited a reverse pattern, first decreasing and then increasing. According to Stokes' law, the rate of particle flotation or sedimentation is influenced by factors such as particle size, the density difference between the particles and the dispersing medium, and the viscosity of the dispersing medium. Consequently, with increasing energy density, the viscosity of the emulsion system also increases. Over the same storage period, this should theoretically result in a thinner fat layer in the upper phase and thus a lower CI. However, at higher energy densities, the CI of PONE increases, suggesting that excessive energy densities may lead to droplet flocculation or the formation of larger aggregates within the emulsion system. This accelerates fat separation and compromises the long-term storage stability of the emulsion. The results indicate that at higher energy densities (1.9 and 2.1 kcal/mL), POBNE

(7.4%, 8.8%) exhibits a lower CI compared to PONE (9.9%, 10.3%). This suggests that POB, as a lipid substitute in emulsions, effectively reduces the rate of fat separation, thereby improving storage stability.

3.1.6 Color analysis

The color analysis results of the emulsions are presented in Table 3. The data indicate that all emulsions exhibited higher L^* and b^* values, suggesting that the overall color of the emulsions was predominantly white with a yellowish hue. Additionally, both

a^* and b^* values increased with rising energy density, indicating a gradual shift in emulsion color toward red and yellow tones. This color change is primarily attributed to the Maillard reaction between sodium caseinate and maltodextrin in the aqueous phase under high-temperature conditions, resulting in the formation of brown reaction products. Furthermore, as the concentrations of

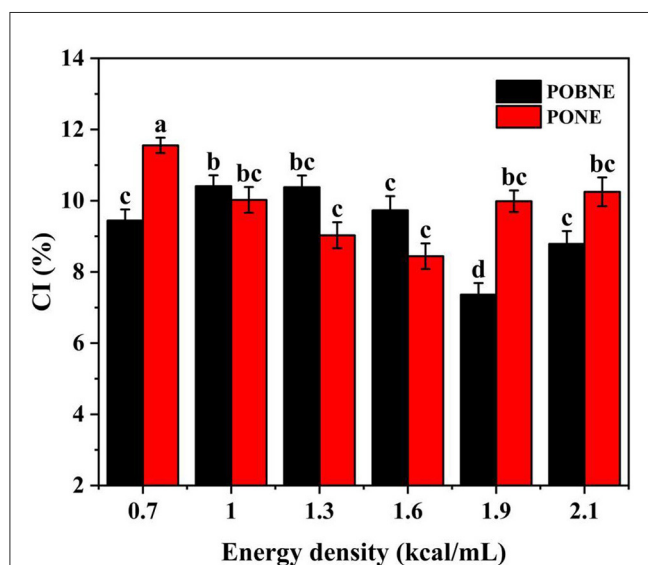


FIGURE 6 Creaming index (CI) of nutritional emulsion at different energy densities after 15 days storage. POBNE, peanut oil body nutritional emulsion; PONE, peanut oil nutritional emulsion. Different letters indicate significant differences ($p < 0.05$).

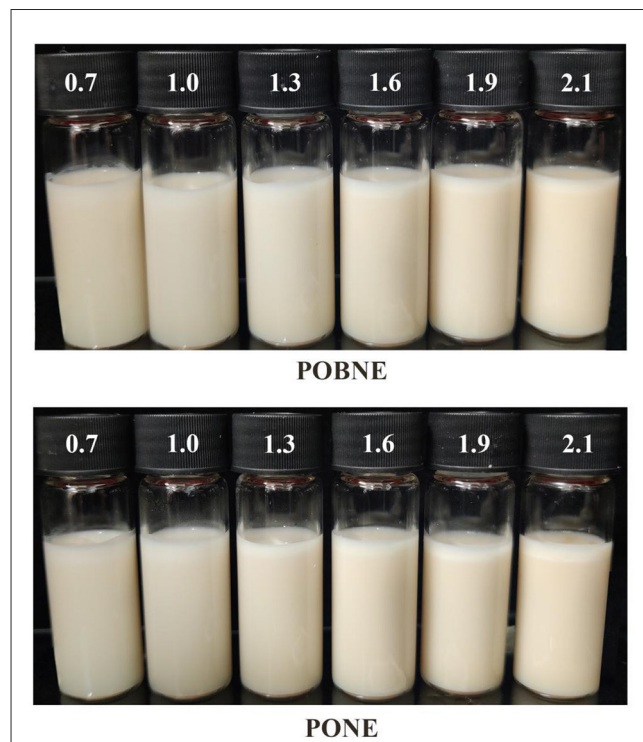


FIGURE 7 Appearance of nutritional emulsions at different energy densities. POBNE, peanut oil body nutritional emulsion; PONE, peanut oil nutritional emulsion. Different numbers represent energy density, kcal/mL.

TABLE 3 Color properties of nutritional emulsion at different energy densities.

Sample	Energy density (kcal/mL)	L^*	a^*	b^*	ΔE^*
POBNE	0.7	64.37 ± 0.24 ^b	2.91 ± 0.01 ^f	9.83 ± 0.02 ^e	29.41 ± 0.24 ^c
	1.0	64.43 ± 0.06 ^b	3.23 ± 0.01 ^e	10.59 ± 0.03 ^d	29.56 ± 0.04 ^c
	1.3	64.50 ± 0.15 ^b	3.49 ± 0.03 ^d	10.74 ± 0.02 ^d	29.55 ± 0.14 ^c
	1.6	62.43 ± 0.14 ^c	4.18 ± 0.01 ^c	12.12 ± 0.03 ^c	31.98 ± 0.13 ^b
	1.9	61.66 ± 0.05 ^d	4.40 ± 0.03 ^b	12.60 ± 0.07 ^b	32.87 ± 0.06 ^a
	2.1	69.09 ± 0.06 ^a	5.37 ± 0.01 ^a	13.58 ± 0.02 ^a	26.43 ± 0.06 ^d
PONE	0.7	63.52 ± 0.31 ^c	3.57 ± 0.04 ^f	9.36 ± 0.03 ^f	30.22 ± 0.31 ^d
	1.0	72.34 ± 0.03 ^a	4.55 ± 0.02 ^e	11.16 ± 0.02 ^e	22.43 ± 0.03 ^f
	1.3	61.86 ± 0.23 ^d	5.14 ± 0.02 ^d	11.67 ± 0.04 ^d	32.54 ± 0.23 ^c
	1.6	61.21 ± 0.02 ^e	5.31 ± 0.01 ^c	12.19 ± 0.01 ^c	33.33 ± 0.01 ^b
	1.9	60.25 ± 0.05 ^f	5.35 ± 0.01 ^b	12.76 ± 0.04 ^b	34.40 ± 0.05 ^a
	2.1	67.06 ± 0.05 ^b	6.14 ± 0.03 ^a	13.95 ± 0.02 ^a	28.57 ± 0.05 ^e

POBNE, peanut oil body nutritional emulsion; PONE, peanut oil nutritional emulsion. Values are expressed as the mean ± SD. Different letters in the same column indicate significant differences ($p < 0.05$).

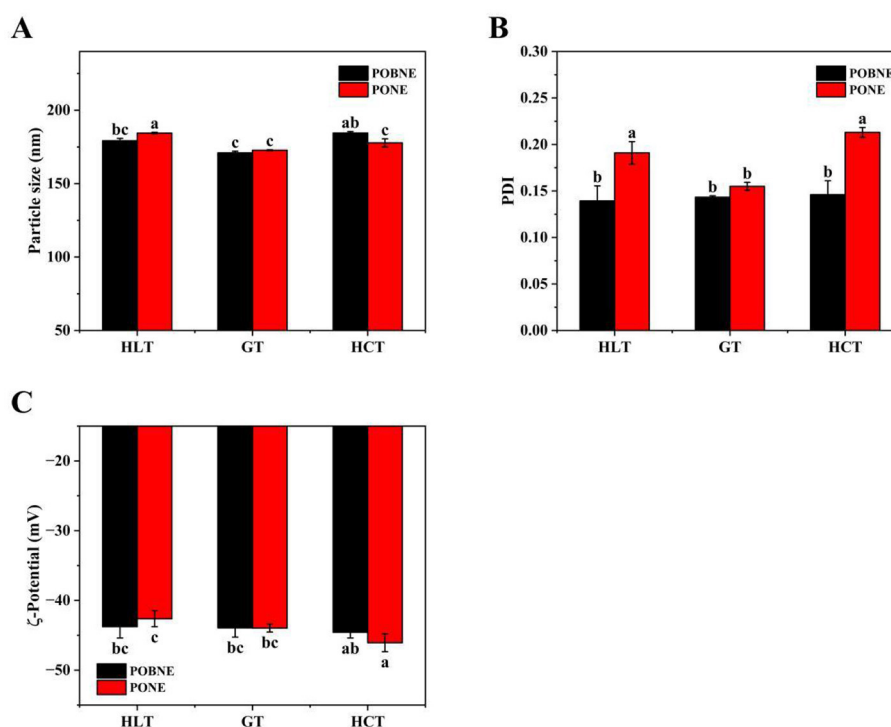


FIGURE 8 Volume average particle size (A), polymer dispersity index (PDI) (B) and ζ -potential (C) of nutritional emulsion at different nutrient ratios. POBNE, peanut oil body nutritional emulsion; PONE, peanut oil nutritional emulsion; HLT, high lipid type; GT, general type; HCT, high carbohydrate type. Different letters indicate significant differences ($p < 0.05$).

protein and polysaccharide in the emulsion system increase, the Maillard reaction rate accelerates, leading to a higher production of browning compounds and a darker emulsion color (Dursun Capar and Yalcin, 2021). However, at the same energy density, POBNE generally exhibited lower a^* and b^* values compared to PONE, indicating lighter colors and potentially higher sensory acceptance. This is more intuitively illustrated in Figure 7, which shows the color of the emulsions.

3.2 Effect of nutrient ratio on emulsion properties

To address specific nutritional requirements, this section investigates the effect of nutrient ratio on the properties of nutritional emulsion at an energy density of 2.1 kcal/mL.

3.2.1 Particle size and ζ -potential

The particle size results of each emulsion are shown in Figure 8A. Under the HLT formulation, the particle size of POBNE (174.2 nm) was significantly smaller than that of PONE (184.5 nm; $p < 0.05$). In contrast, under the HCT formulation, the particle size of POBNE (184.5 nm) was significantly larger than that of PONE (177.8 nm; $p < 0.05$). These results indicate that the nutritional emulsion prepared with POB exhibited better stability at higher lipid content under the same energy density.

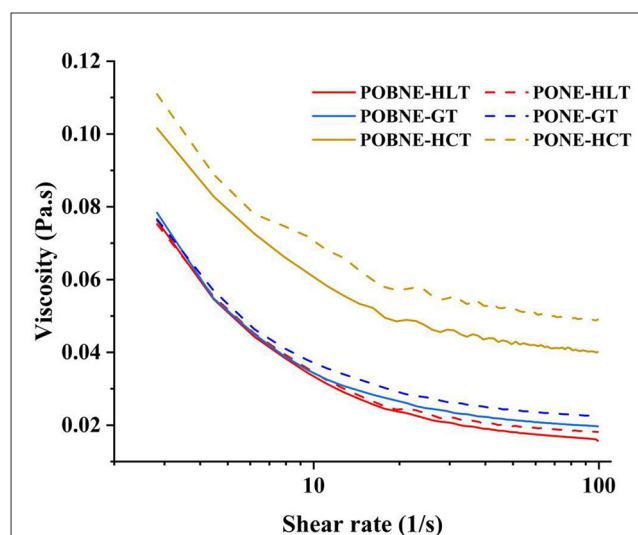


FIGURE 9 Apparent viscosity of nutritional emulsions at different nutrient ratios as a function of shear rate (1–100 1/s). POBNE, peanut oil body nutritional emulsion; PONE, peanut oil nutritional emulsion; HLT, high lipid type; GT, general type; HCT, high carbohydrate type.

This may be attributed to the increased lipid content, which promotes the participation of oleosin and phosphatidylcholine in emulsification, thereby reducing the interfacial tension at the oil-water interface and facilitating the formation of smaller droplets

(Yang et al., 2025). Figure 8B shows the PDI values of the emulsions under different nutrient ratios. The POBNE consistently exhibited lower PDI values compared to PONE, suggesting that the droplets formed by POBNE were more uniform, stable, and better dispersed. Figure 8C illustrates the ζ -potential of the emulsions. The POBNE in the HLT group showed a higher absolute ζ -potential value, while the POBNE in the HCT group exhibited a lower absolute ζ -potential value. These findings suggest that at higher lipid content, the emulsion droplets prepared with POB had stronger electrostatic interactions, contributing to a more stable emulsion system. This conclusion aligns with the particle size results.

3.2.2 Apparent viscosity

The apparent viscosity of the emulsions as a function of shear rate ($1\text{--}100\text{ s}^{-1}$) is shown in Figure 9. With increasing shear rate, all emulsion groups exhibited shear-thinning behavior, suggesting that droplet deformation occurs during the shear process. The results showed that the PONE in the HCT group exhibited the highest apparent viscosity (0.11 Pa.s). This phenomenon can be explained by two main factors. First, the emulsion contains a higher concentration of maltodextrin, which acts as a strong thickening agent, thereby reducing its fluidity. Second, the emulsifier may promote the formation of larger droplet aggregates, resulting in a more viscous emulsion (Pan et al., 2025). In contrast, the apparent viscosities of the GT and HLT nutritional emulsions were relatively low, and the viscosity curves of POBNE and PONE were nearly identical. This indicates that the POBNE under the GT and HCT formulation exhibited rheological properties similar to those of emulsions prepared with traditional emulsifiers.

3.2.3 Storage stability

The TSI of each emulsion is shown in Figure 10. The results showed that the TSI of each emulsion was below 0.3, indicating excellent stability for emulsions with all three nutrient ratios in both the POBNE and PONE systems. In the POBNE system, the terminal TSI at the end of the scan was lowest for HCT, highest for GT, and intermediate for HLT. Conversely, in the PONE system, the terminal TSI at the end of the scan was lowest for HCT, highest for HLT, and intermediate for GT. For HLT and HCT emulsions, the TSI at the end of the scan was lower in the POBNE system than in the PONE system, whereas for GT, the TSI was higher in the POBNE system than in the PONE system. In addition, CI results demonstrated that all emulsion exhibited varying degrees of stratification, as shown in the Figure 11. Under the HLT formulation, POBNE (8.79%) and PONE (10.25%) had higher CI, indicating a more pronounced phenomenon of fat floating and stratification. This can be attributed to the high lipid content in these emulsions, which increases the number of oil droplets in the system and accelerates the formation of thicker, more distinct layers. In contrast, the emulsions under the GT and HCT formulation showed no significant difference in CI ($p > 0.05$). This may be due to the density difference between the oil phase and the water phase. Oil droplets, having a lower density, tend to rise toward the denser water phase, leading to stratification. The rate of this stratification is influenced by the magnitude of the density difference. Under the HCT formulation, the high maltodextrin concentration increases the density of the water phase, thereby accelerating the upward movement of oil droplets. Conversely, emulsions under the GT formulation, despite their higher lipid content, have a lower maltodextrin concentration, which results in a lower water phase density and slows the flotation of oil droplets. As a result, the CI of emulsions under GT and HCT formulation are similar. Additionally, across

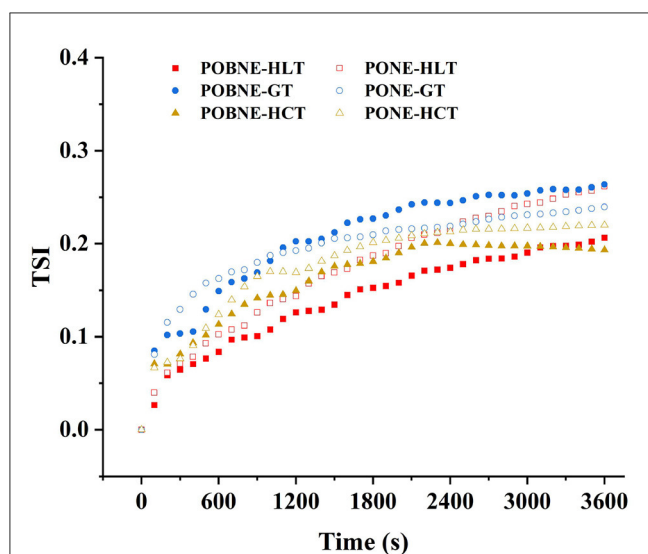


FIGURE 10
Turbiscan stability index (TSI) of nutritional emulsion at different nutrient ratios. POBNE, peanut oil body nutritional emulsion; PONE, peanut oil nutritional emulsion; HLT, high lipid type; GT, general type; HCT, high carbohydrate type.

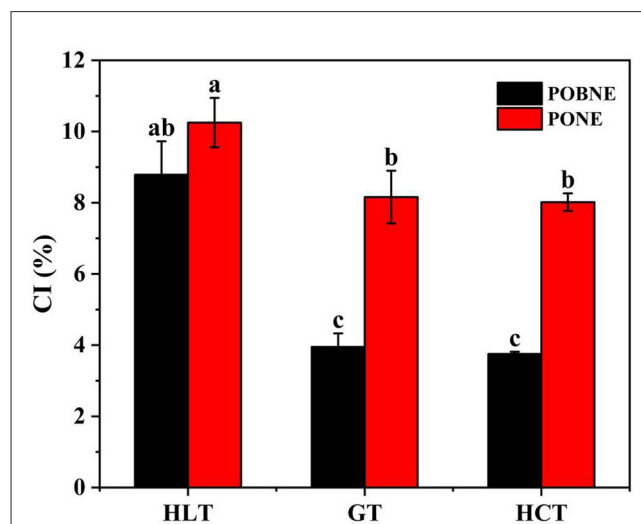


FIGURE 11
Creaming index (CI) of nutritional emulsion at different nutrient ratios stored for 15 days. POBNE, peanut oil body nutritional emulsion; PONE, peanut oil nutritional emulsion; HLT, high lipid type; GT, general type; HCT, high carbohydrate type. Different letters indicate significant differences ($p < 0.05$).

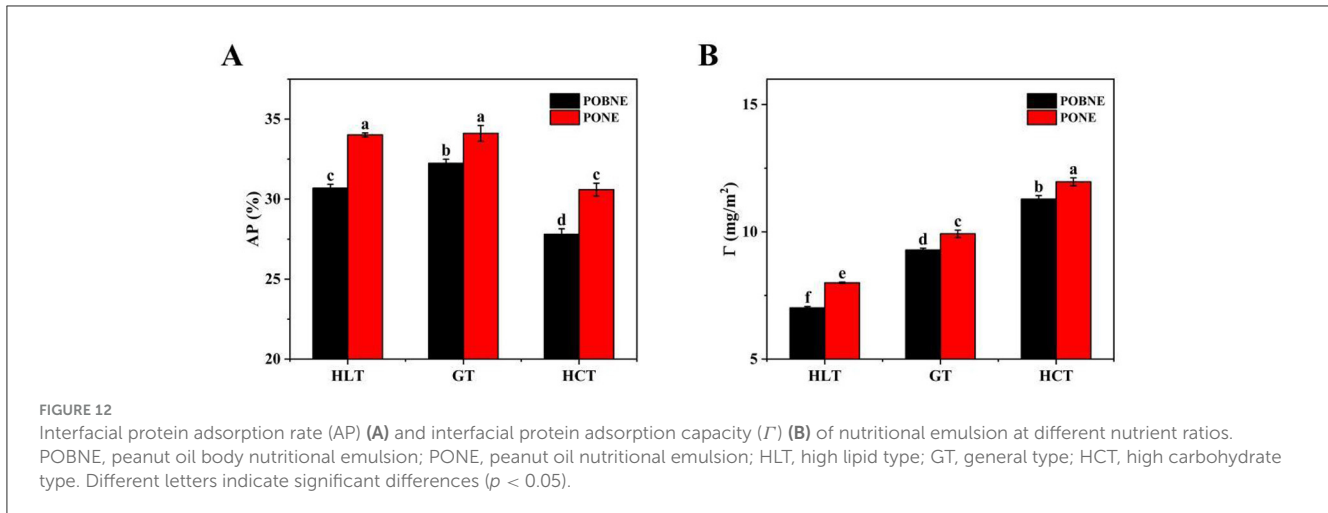


TABLE 4 Color properties of nutritional emulsion at different nutrient ratios.

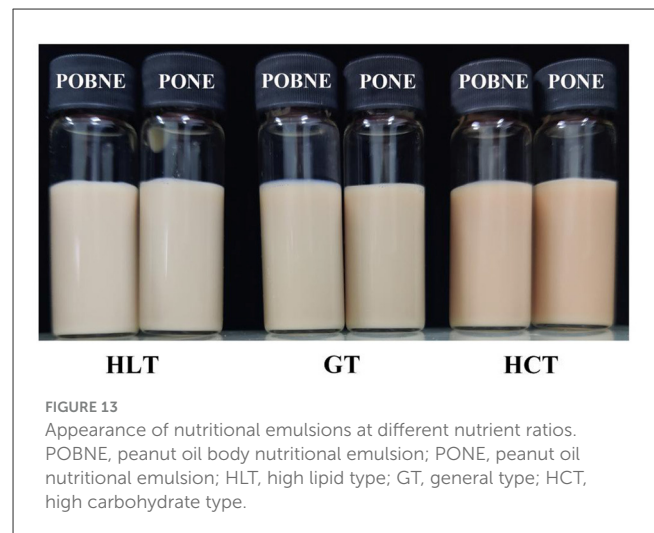
Sample	Type	L^*	a^*	b^*	ΔE^*
POBNE	HLT	69.1 ± 0.06 ^a	5.4 ± 0.01 ^f	13.6 ± 0.02 ^d	26.4 ± 0.06 ^f
	GT	64.7 ± 0.03 ^d	6.0 ± 0.03 ^e	15.3 ± 0.03 ^b	31.2 ± 0.04 ^d
	HCT	69.0 ± 0.07 ^a	8.3 ± 0.02 ^b	11.5 ± 0.02 ^f	48.9 ± 0.06 ^a
PONE	HLT	67.1 ± 0.05 ^b	6.1 ± 0.03 ^d	13.9 ± 0.03 ^c	28.6 ± 0.05 ^e
	GT	62.5 ± 0.04 ^e	6.8 ± 0.01 ^c	15.6 ± 0.02 ^a	33.4 ± 0.03 ^c
	HCT	65.4 ± 0.06 ^c	8.5 ± 0.01 ^a	12.8 ± 0.03 ^c	45.8 ± 0.06 ^b

POBNE, peanut oil body nutritional emulsion; PONE, peanut oil nutritional emulsion. Values are expressed as the mean ± SD. Different letters in the same column indicate significant differences ($p < 0.05$).

different nutrient ratios, POBNE consistently exhibited lower CI than PONE, suggesting that emulsions prepared with POB have better storage stability and can delay oil droplet flotation. This could be attributed to the presence of oleosin in the droplets, which reduces the tendency for coalescence and helps maintain smaller particle sizes.

3.2.4 Interface protein of emulsion

The AP values of each emulsion are shown in [Figure 12A](#). The results indicate that emulsions under HLT and GT formulation exhibited higher AP values, while the HCT group showed lower AP values. This difference may be attributed to the lipid content of the emulsions. Under HCT formulation, the lower lipid content results in fewer droplets in the homogenized emulsion, leading to a smaller total surface area and a reduction in adsorbed proteins ([Ravera et al., 2021](#)). Additionally, the AP values of POBNE (30.69%, 32.24%, and 27.8% for HLT, GT, and HCT, respectively) were consistently lower than those of PONE (34.01%, 34.11%, and 30.59% for HLT, GT, and HCT, respectively). This suggests that emulsions prepared with POB require less protein for emulsification, as the protein at the oil-water interface reaches saturation more quickly, contributing to improved emulsion stability.



The Γ values of each emulsion are presented in [Figure 12B](#). The Γ values of both POBNE and PONE increased progressively from the HLT formulation to the GT formulation and then to the HCT formulation. This trend may be explained by the lower lipid content in the HCT emulsions, which results in fewer droplets and reduces the likelihood of droplet friction and collision, making it more

difficult for adsorbed proteins to detach. On the other hand, with the increase of maltodextrin content, the viscosity of the emulsion increases, the Brownian motion of the droplets is suppressed, and more proteins can be retained at the oil-water interface (Karim et al., 2024). In addition, the Γ values of POBNE (7.01, 9.29, and 11.29 mg/m² for HLT, GT, and HCT, respectively) were lower than those of PONE (8.00, 9.92, and 11.96 mg/m² for HLT, GT, and HCT, respectively). This indicates that POBNE forms a thinner protein layer at the oil-water interface.

3.2.5 Color analysis

The color analysis results of each emulsion are presented in Table 4. The results indicate that both a^* and b^* values of the emulsions are positive, with b^* values being significantly higher. This suggests that red and yellow are the dominant colors of the emulsions, with yellow being more pronounced. The observed color changes are primarily attributed to the Maillard reaction between proteins and polysaccharides in the emulsion during high-temperature sterilization, which produces brown reaction products and alters the emulsion's color. Among them, the HCT emulsions exhibited the highest ΔE^* value, indicating more significant color changes. This phenomenon can be attributed to two main factors. First, the HCT emulsions exhibit a lower protein adsorption rate, resulting in a higher concentration of free proteins and amino compounds in the water phase. Second, the higher maltodextrin content in the HCT emulsions contributes to an increased concentration of carbonyl compounds in the water phase. The abundance of amino and carbonyl compounds intensifies the Maillard reaction in the HCT emulsions, resulting in the formation of more brown products. Additionally, compared to PONE, POBNE still exhibits smaller a^* and b^* values, indicating that POBNE has higher sensory acceptance. The appearance and color differences of the emulsions can be observed more directly in Figure 13.

4 Conclusion

In conclusion, the nutritional emulsion prepared using POB demonstrates significant advantages over traditional nutritional emulsions made with emulsifiers. The natural oleosin and phospholipids in OB interact with sodium caseinate at the oil droplet interface to form a high-performance interfacial film. Under conditions of higher energy density, POBNE exhibits better dispersion and stronger anti-coalescence properties. Furthermore, POBNE requires less adsorbed protein to achieve stability and maintains superior storage stability even with a thinner interfacial film. Notably, POBNE with an energy density of 2.1 kcal/mL continues to exhibit better emulsion characteristics than PONE, even when the nutrient ratio is adjusted. These findings suggest that OB can serve as an effective alternative emulsification system in food formulations, offering a promising approach to developing healthy nutritional emulsion foods without added emulsifiers. Future research should focus on exploring the interactions between various nutrients in OB-based emulsions and investigating their effects on human digestion and absorption. Such studies will

provide deeper insights into the potential applications of OB in functional and health-oriented food products.

Data availability statement

The original contributions presented in the study are included in the article/supplementary material, further inquiries can be directed to the corresponding authors.

Author contributions

ZL: Writing – original draft, Investigation, Writing – review & editing. ZZ: Conceptualization, Funding acquisition, Writing – review & editing. PZ: Methodology, Writing – original draft, Investigation. YD: Methodology, Writing – original draft. GL: Writing – review & editing, Supervision. PL: Writing – review & editing, Software. JZ: Formal analysis, Writing – review & editing. FX: Validation, Writing – review & editing. JP: Conceptualization, Writing – review & editing, Project administration. MZ: Conceptualization, Project administration, Writing – review & editing.

Funding

The author(s) declare that financial support was received for the research and/or publication of this article. This work was supported by National Natural Science Foundation of China (U22A20539), Fujian Key Laboratory of Agro-products Quality & Safety (APQSKF202304), and the Special Fund for Scientific Innovation Strategy-Construction of high level academy of Agriculture Science (R2021YJ-YB2001/R2023PY-QF002).

Conflict of interest

The authors declare that the research was conducted in the absence of any commercial or financial relationships that could be construed as a potential conflict of interest.

Generative AI statement

The author(s) declare that no Gen AI was used in the creation of this manuscript.

Publisher's note

All claims expressed in this article are solely those of the authors and do not necessarily represent those of their affiliated organizations, or those of the publisher, the editors and the reviewers. Any product that may be evaluated in this article, or claim that may be made by its manufacturer, is not guaranteed or endorsed by the publisher.

References

- Abu-Qare, A., Elmasy, E., and Abou-Donia, M. (2003). A role for p-glycoprotein in environmental toxicology. *J. Toxicol. Environ. Heal. Part B* 6, 279–288. doi: 10.1080/10937400306466
- Arancibia, C., Riquelme, N., Zúñiga, R., and Matiacevich, S. (2017). Comparing the effectiveness of natural and synthetic emulsifiers on oxidative and physical stability of avocado oil-based nanoemulsions. *Innov. Food Sci. Emerg. Technol.* 44, 159–166. doi: 10.1016/j.ifset.2017.06.009
- Bonsegna, S., Bettini, S., Pagano, R., Zacheo, A., Vergaro, V., Giovinazzo, G., et al. (2011). Plant oil bodies: novel carriers to deliver lipophilic molecules. *Appl. Biochem. Biotechnol.* 163, 792–802. doi: 10.1007/s12010-010-9083-0
- Cawood, A. L., Elia, M., and Stratton, R. J. (2012). Systematic review and meta-analysis of the effects of high protein oral nutritional supplements. *Ageing Res. Rev.* 11, 278–296. doi: 10.1016/j.arr.2011.12.008
- Chassaing, B., Koren, O., Goodrich, J. K., Poole, A. C., Srinivasan, S., Ley, R. E., et al. (2015). Dietary emulsifiers impact the mouse gut microbiota promoting colitis and metabolic syndrome. *Nature* 519, 92–96. doi: 10.1038/nature14232
- Csáki, K. F. (2011). Synthetic surfactant food additives can cause intestinal barrier dysfunction. *Med. Hypotheses* 76, 676–681. doi: 10.1016/j.mehy.2011.01.030
- Diao, X., Jia, R., Wang, Y., Liu, G., Chen, X., Liu, D., et al. (2024). The physicochemical properties, microstructure, and stability of diacylglycerol-loaded multilayer emulsion based on protein and polysaccharides. *LWT* 196:115879. doi: 10.1016/j.lwt.2024.115879
- Dou, N., Sun, R., Su, C., Ma, Y., Zhang, X., Wu, M., et al. (2022). Soybean oil bodies as a milk fat substitute improves quality, antioxidant and digestive properties of yogurt. *Food* 11:2088. doi: 10.3390/foods11142088
- Dursun Capar, T., and Yalcin, H. (2021). Protein/polysaccharide conjugation via Maillard reactions in an aqueous media: impact of protein type, reaction time and temperature. *LWT* 152:112252. doi: 10.1016/j.lwt.2021.112252
- Furuta, R., Hatao, F., Itokawa, M., Yamazaki, R., Morikawa, Y., Honda, M., et al. (2023). Feasibility and safety of super energy-dense oral nutritional supplementation in postoperative gastric cancer patients. *Cancer Diagnosis Progn.* 3, 514–521. doi: 10.21873/cdp.10248
- Gao, Y., Zheng, Y., Yao, F., and Chen, F. (2022). Effects of pH and temperature on the stability of peanut oil bodies: new insights for embedding active ingredients. *Colloids Surfaces A Physicochem. Eng. Asp.* 654:130110. doi: 10.1016/j.colsurfa.2022.130110
- Guzha, A., Whitehead, P., Ischebeck, T., and Chapman, K. D. (2023). Lipid droplets: packing hydrophobic molecules within the aqueous cytoplasm. *Annu. Rev. Plant Biol.* 74, 195–223. doi: 10.1146/annurev-arplant-070122-021752
- Kang, Z.-L., Xie, J., Hu, Z., Li, Y., and Ma, H.-J. (2023). Effect of safflower oil and magnetic field-modified soy 11S globulin on rheological and emulsifying properties of oil-in-water emulsions. *Food Hydrocoll.* 142:108775. doi: 10.1016/j.foodhyd.2023.108775
- Karim, A., Mohammadi, L., Osse, E. F., Aider, M., Saqui-Salces, M., and Khalloufi, S. (2024). Effect of polysaccharide-induced viscosity on the digestion of proteins, fats, and carbohydrates in food: a comprehensive review and future perspectives. *Trends Food Sci. Technol.* 153:104757. doi: 10.1016/j.tifs.2024.104757
- Kim, W., Wang, Y., and Selomulya, C. (2020). Dairy and plant proteins as natural food emulsifiers. *Trends Food Sci. Technol.* 105, 261–272. doi: 10.1016/j.tifs.2020.09.012
- Kong, Y., Chen, J., Hong, Z., Guo, R., and Huang, Q. (2025). Insights into the Pickering emulsions stabilized by yeast dietary fiber: interfacial adsorption kinetics, rheological characteristics, and stabilization mechanisms. *Food Chem.* 464:141924. doi: 10.1016/j.foodchem.2024.141924
- Lerner, A., and Matthias, T. (2015). Changes in intestinal tight junction permeability associated with industrial food additives explain the rising incidence of autoimmune disease. *Autoimmun. Rev.* 14, 479–489. doi: 10.1016/j.autrev.2015.01.009
- Li, D., Zhao, Y., Wang, X., Tang, H., Wu, N., Wu, F., et al. (2020). Effects of (+)-catechin on a rice bran protein oil-in-water emulsion: droplet size, zeta-potential, emulsifying properties, and rheological behavior. *Food Hydrocoll.* 98:105306. doi: 10.1016/j.foodhyd.2019.105306
- Lin, Z., Zhou, P., Deng, Y., Liu, G., Li, P., Zeng, J., et al. (2025). Impact of homogenization methods on the interfacial protein composition and stability of peanut oil body emulsion with sodium caseinate and maltodextrin. *LWT* 215:117286. doi: 10.1016/j.lwt.2024.117286
- Liu, Y., Wu, Q., Zhang, J., Yan, W., and Mao, X. (2024). Food emulsions stabilized by proteins and emulsifiers: a review of the mechanistic explorations. *Int. J. Biol. Macromol.* 261:129795. doi: 10.1016/j.ijbiomac.2024.129795
- McClements, D. J., Bai, L., and Chung, C. (2017). Recent advances in the utilization of natural emulsifiers to form and stabilize emulsions. *Annu. Rev. Food Sci. Technol.* 8, 205–236. doi: 10.1146/annurev-food-030216-030154
- Mert, B., and Vilgis, T. A. (2021). Hydrocolloid coated oleosomes for development of oleogels. *Food Hydrocoll.* 119:106832. doi: 10.1016/j.foodhyd.2021.106832
- Pan, R., Iqbal, S., Wang, N., Wu, P., Chen, H., Bhutto, R. A., et al. (2025). Alteration in rheological and digestive properties of O/W emulsions using controlled aggregation of konjac glucomannan and xanthan gum in aqueous phases. *Food Hydrocoll.* 160:110795. doi: 10.1016/j.foodhyd.2024.110795
- Qu, D., Bo, P., Li, Z., and Sun, Y. (2024). Effects of whole nutritional formula foods on nutritional improvement and intestinal flora in malnourished rats. *Food Sci. Nutr.* 12, 1724–1735. doi: 10.1002/fsn3.3865
- Ravera, F., Dziza, K., Santini, E., Cristofolini, L., and Liggieri, L. (2021). Emulsification and emulsion stability: the role of the interfacial properties. *Adv. Colloid Interface Sci.* 288:102344. doi: 10.1016/j.cis.2020.102344
- Ren, C., Xiong, W., Peng, D., He, Y., Zhou, P., Li, J., et al. (2018). Effects of thermal sterilization on soy protein isolate/phyenol complexes: aspects of structure, in vitro digestibility and antioxidant activity. *Food Res. Int.* 112, 284–290. doi: 10.1016/j.foodres.2018.06.034
- Schröder, A., Berton-Carabin, C., Venema, P., and Cornacchia, L. (2017). Interfacial properties of whey protein and whey protein hydrolysates and their influence on O/W emulsion stability. *Food Hydrocoll.* 73, 129–140. doi: 10.1016/j.foodhyd.2017.06.001
- Shen, P., Wu, J., Zhao, M., and Zhou, F. (2024). Does particle size matter for soy protein nanoparticles in the fabrication and lipolysis of pickering-like emulsions? *Food Hydrocoll.* 153:110005. doi: 10.1016/j.foodhyd.2024.110005
- Shi, Z., Li, K., and Meng, Z. (2024). Recent trends in oleosomes: extraction methods, structural characterization, and novel applications. *Trends Food Sci. Technol.* 151:104621. doi: 10.1016/j.tifs.2024.104621
- Sun, Y., Zhong, M., Liao, Y., Kang, M., Li, Y., and Qi, B. (2023). Interfacial characteristics of artificial oil body emulsions (O/W) prepared using extrinsic and intrinsic proteins: inspired by natural oil body. *LWT* 173:114270. doi: 10.1016/j.lwt.2022.114270
- Wali, J. A., Ni, D., Raubenheimer, D., and Simpson, S. J. (2025). Macronutrient interactions and models of obesity: insights from nutritional geometry. *BioEssays* 47:e2400071. doi: 10.1002/bies.202400071
- Yamazaki, R., Hatao, F., Itokawa, M., Morikawa, Y., Honda, M., Imamura, K., et al. (2023). Impact of super energy-dense oral nutritional supplementation (SED ONS) on glycemic variability and food intake postoperatively in gastric cancer patients. *Surg. Today* 53, 605–613. doi: 10.1007/s00595-022-02600-w
- Yang, J., Fan, H., Jiang, B., Li, R., Fan, J., Li, B., et al. (2023). Excipient emulsion prepared with pectin and sodium caseinate to improve the bioaccessibility of carotenoids in mandarin juice: the effect of emulsifier and polymer concentration. *Food Chem. X* 20:100909. doi: 10.1016/j.fochx.2023.100909
- Yang, J., Plankensteiner, L., de Groot, A., Hennebel, M., Sagis, L. M. C., and Nikiforidis, C. V. (2025). The role of oleosins and phosphatidylcholines on the membrane mechanics of oleosomes. *J. Colloid Interface Sci.* 678, 1001–1011. doi: 10.1016/j.jcis.2024.09.171
- Yu, M.-J., Feng, R., Long, S., Tao, H., and Zhang, B. (2025). Stabilizing emulsions by ultrasound-treated pea protein isolate - tannic acid complexes: impact of ultrasonic power and concentration of complexes on emulsion characteristics. *Food Chem.* 463:141266. doi: 10.1016/j.foodchem.2024.141266
- Yu, Q., Wu, H., and Fan, L. (2024). Formation of casein and maltodextrin conjugates using shear and their effect on the stability of total nutrient emulsion based on homogenization. *Food Hydrocoll.* 149:109533. doi: 10.1016/j.foodhyd.2023.109533
- Yuan, X., Wei, Y., Jiang, H., Wang, H., Wang, Z., Dong, M., et al. (2024). Longitudinal relationship between the percentage of energy intake from macronutrients and overweight/obesity among Chinese adults from 1991 to 2018. *Nutrients* 16:666. doi: 10.3390/nu16050666
- Zaaboul, F., Tian, T., Borah, P. K., and Di Bari, V. (2024). Thermally treated peanut oil bodies as a fat replacer for ice cream: physicochemical and rheological properties. *Food Chem.* 436:137630. doi: 10.1016/j.foodchem.2023.137630
- Zaaboul, F., Zhao, Q., Xu, Y., and Liu, Y. (2022). Soybean oil bodies: a review on composition, properties, food applications, and future research aspects. *Food Hydrocoll.* 124:107296. doi: 10.1016/j.foodhyd.2021.107296
- Zhang, M., Fan, L., Liu, Y., Huang, S., and Li, J. (2022). Effects of proteins on emulsion stability: the role of proteins at the oil–water interface. *Food Chem.* 397:133726. doi: 10.1016/j.foodchem.2022.133726
- Zhang, X., Zhang, S., Xie, F., Han, L., Li, L., Jiang, L., et al. (2021). Soy/whey protein isolates: interfacial properties and effects on the stability of oil-in-water emulsions. *J. Sci. Food Agric.* 101, 262–271. doi: 10.1002/jsfa.10638